

The Δ -resonance in a finite volume^{#1}

Véronique Bernard^{a,#2}, Ulf-G. Meißner^{b,c,#3} and Akaki Rusetsky^{b,d,#4}

^a*Université Louis Pasteur, Laboratoire de Physique Théorique
3-5, rue de l'Université, F-67084 Strasbourg, France*

^b*Universität Bonn, Helmholtz-Institut für Strahlen- und Kernphysik (Theorie)
Nußallee 14-16, D-53115 Bonn, Germany*

^c*Forschungszentrum Jülich, Institut für Kernphysik (Theorie)
D-52425 Jülich, Germany*

^d*On leave of absence from: High Energy Physics Institute,
Tbilisi State University, University St. 9, 380086 Tbilisi, Georgia*

Abstract

We study the extraction of Δ -resonance parameters from lattice data for small quark masses, corresponding to the case of an unstable Δ . To this end, we calculate the spectrum of the correlator of two Δ -fields in a finite Euclidian box up-to-and-including $O(\epsilon^3)$ in the small scale expansion using infrared regularization. On the basis of our numerical study, we argue that the extraction of the parameters of the Δ -resonance (in particular, of the mass and the pion-nucleon-delta coupling constant) from the measured volume dependence of the lowest energy levels should be feasible.

Pacs: 12.38.Gc, 12.39.Fe, 11.10.St

Keywords: Lattice QCD, Baryon resonances, Chiral Lagrangians, Field theory in a finite volume

^{#1}This research is part of the EU Integrated Infrastructure Initiative Hadron Physics Project under contract number RII3-CT-2004-506078. Work supported in part by DFG (SFB/TR 16, "Subnuclear Structure of Matter") and by the EU Contract No. MRTN-CT-2006-035482, "FLAVIANet".

^{#2}email: bernard@lpt6.u-strasbg.fr

^{#3}email: meissner@itkp.uni-bonn.de

^{#4}email: rusetsky@itkp.uni-bonn.de

1 Introduction

Monte-Carlo simulations in lattice QCD enable one to calculate the spectrum of low-lying hadrons from first principles and thus to obtain important information about the long-range dynamics of quarks and gluons. In the past, a major effort has been concentrated on the study of the ground-state particle spectrum. However, recently there has been a lot of work on the spectroscopy of the excited nucleon states as well [1–9]. For the status of lattice calculations of the baryon spectrum, see e.g. the recent reviews [10, 11]. We note that several long-standing puzzles in the field are still awaiting a resolution. In particular, it is worth to mention the problem of the level ordering of the negative-parity nucleon excitation N^* (1535) and the positive-parity Roper resonance N^* (1440) as well as the structure of the Λ (1405).

The Δ -resonance is the most important baryon resonance. Its mass is close to the mass of the nucleon, and it couples strongly to nucleons, pions and photons. It is clear that a systematic study of the properties of the Δ -resonance in lattice QCD could lay a solid theoretical basis for understanding the low-energy QCD dynamics in the one-baryon sector in lattice QCD. Evaluating the mass of the Δ -resonance has already been addressed in the last few years. For illustration, we consider the recent calculation of the Δ -mass in quenched QCD using a tadpole-improved anisotropic action and FLIC fermions [8]. In this paper, the local interpolating field with quantum numbers of the Δ^+ has been chosen in the following manner

$$\chi_\mu = \frac{1}{\sqrt{3}} \epsilon_{abc} \left\{ 2(u^{aT} C \gamma_\mu d^b) u^c + (u^{aT} C \gamma_\mu u^b) d^c \right\}, \quad (1)$$

where a, b, c denote color indices and C is the charge conjugation matrix. With this interpolating field one further calculates the two-point correlation function at zero spatial momentum and at large Euclidean time, extracting the mass spectrum. More precisely, in Ref. [8] the calculation of the ratio m_Δ/m_N (as well as the similar ratios for some other excited baryon states) has been performed down to the quark masses corresponding to $(M_\pi/M_\rho)^2 = 0.4$. At such quark masses, the dependence of the data on $(M_\pi/M_\rho)^2$ is very smooth (almost linear). However, a large gap in the quark (pion) mass has still to be bridged if the data are extrapolated down to the physical value of $(M_\pi/M_\rho)^2 \simeq 0.03$.

The above example highlights all features of the lattice calculations of the parameters of baryon resonances (and the Δ -resonance, in particular), which we wish to put under scrutiny in the present paper:

- a) As already mentioned, the distance from the lowest data point to the physical value of the quark mass is still very large and this will lead to large extrapolation errors. In case of a stable particle, one would argue that performing calculations at smaller quark masses will reduce this uncertainty until, eventually, the simulations are done close to or at the physical value of the quark mass. However, in the case of a resonance, the threshold value of the quark mass exists after which e.g. the Δ starts to decay into a pion and a nucleon. It is evident that, below the threshold, the method which was described above can not be applied straightforwardly. Does this mean that, in the case of a resonance, there is *always* a (not so small) gap in the lattice data, where one should rely only on chiral extrapolation?
- b) Lattice data are always real. Does this mean that one gets the real part of the resonance pole mass as a result of a chiral extrapolation below the decay threshold?
- c) Can one determine the decay width of a resonance by combining the method described above with the chiral extrapolation?

Note also that the Monte-Carlo simulations e.g. in Ref. [8] have been carried out in the quenched approximation. It is however clear that unstable systems at small quark masses, which will be considered below, can be meaningfully discussed only in the context of lattice data based on simulations with dynamical fermions.

To summarize, we want to ask whether there exists a modification of the above method that enables one (at least, in principle) to carry out calculations of the properties of an excited state at such quark masses when this state becomes unstable. Moreover, one would like to eventually walk all way down to the physical quark mass, excluding the extrapolation error altogether (like this appears possible for ground-state hadrons). It would also be very instructive to see in detail what happens in the vicinity of the threshold, when one crosses it while performing a chiral extrapolation of the spectrum. Finally, one should investigate which quantities are most sensitive to the resonance parameters at small quark masses, and how accurately one could extract the mass and the width of the resonance by calculating these quantities on the lattice.

The question of identification of hadron resonances on the lattice has already been addressed in the past. For example, we would like to mention the papers [12–19]. In general, the method proposed originally by Lüscher considers the extraction of the two-body scattering phase shifts from the energy levels, calculated in a finite Euclidean box. In particular, the signatures of unstable particles have been studied. It is demonstrated that in the presence of a narrow resonance the dependence of the energy spectrum of the system on the box size L exhibits a very peculiar behavior near the resonance energy, where the so-called “avoided level crossing” takes place, see Fig. 1. Note that usually this name is used to describe an abrupt rearrangement of the structure of the energy levels of a system, which takes place near the resonance energy when the scattering phase passes through $\pi/2$. From Fig. 1 it is clear that the position of a narrow resonance can be readily identified by measuring the energy levels of a system at a finite volume and locating horizontal “plateaus.” Moreover, the minimal distance that separates the energy levels near the avoided crossing, is determined by the decay width of a resonance and, consequently, the latter quantity can be also extracted from the same lattice data. A very nice qualitative discussion of the avoided level crossing is given e.g. in Refs. [15, 16, 20].

An approach, related to the Lüscher’s method, is used in Ref. [20] to study the structure of the energy levels in the two-pion system carrying the quantum numbers of the ρ -meson. To this end, these energy levels are calculated in an effective field theory (EFT) with a phenomenological lowest-order $\rho\pi\pi$ coupling. Furthermore, in Ref. [21] it has been shown that the presence of a narrow excited state above the threshold modifies the simple exponential decay law of the time-sliced two-point function. The decay width within this approach is extracted not from the two-point function, but directly from the decay amplitudes (see also [22, 23]). In addition, we point out the recent investigation [24], where it is proposed to reconstruct the spectral density in the two-point function by using the maximum entropy method. This approach, in principle, also has the capability to address the problem of unstable states in lattice calculations.

Note also that Lüscher’s approach has been recently applied to study nucleon-nucleon phase shifts at low-energy, as well as two-body shallow bound states [25–29]. To this end, in Ref. [25], Lüscher’s master formula which relates the scattering phase shifts to the energy level displacements caused by the NN interaction, is re-derived within a non-relativistic EFT. Note that at large box sizes, which are used in the study of the scattering processes, the characteristic center-of-mass momenta are small and hence working within the non-relativistic EFT is justified.

An approach, which we use in the present paper, is closely related to the one of Refs. [12–16, 20]. To be precise, we investigate the energy levels of the system with the quantum numbers of the Δ -resonance in a finite box with the size L . This is achieved by calculating the self-energy of the Δ in the

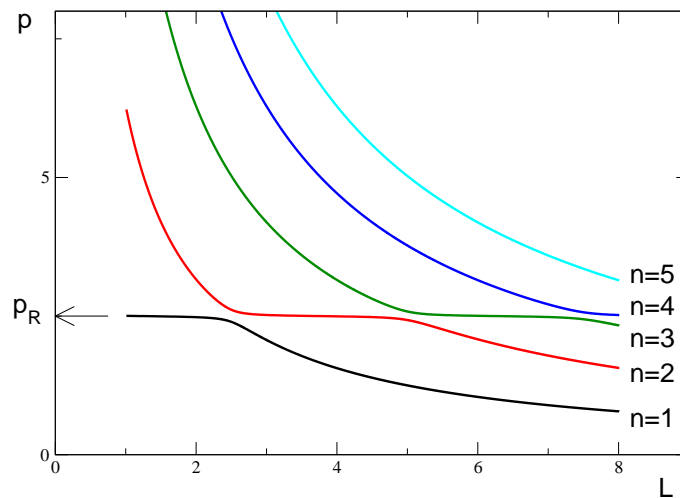


Figure 1: A schematic representation of the avoided level crossing in the presence of a narrow resonance. The center-of-mass momentum of a two-particle pair is plotted against the size of a box L (arbitrary units). It is seen that in the vicinity of the resonance momentum p_R a peculiar behavior of the energy levels is observed. The exact position of the resonance in this case could be easily pinned down by measuring the energy levels on the lattice.

small scale expansion (SSE)^{#5} at a finite volume and finding the poles of the propagator, which yields the parameterization of the spectrum of the Hamiltonian in a finite Euclidean box as a function of the variables M_π and L , as well as the physical masses $m_\Delta(M_\pi)$, $m_N(M_\pi)$ and the $\pi N\Delta$ coupling constant, denoted $g_{\pi N\Delta}$. We further investigate the behavior of energy levels with respect to these parameters. The main question which is addressed here is whether the dependence of the energy levels on the above-mentioned parameters is pronounced enough in order to enable one to perform an accurate fit to determine the mass and width of the Δ -resonance. Here we would like to mention that, as it turns out later, the width of Δ is so large that the avoided level crossing is almost completely washed out from the energy spectrum. Therefore, the nice procedure shown in Fig. 1 does not immediately apply and, in order to be able to accurately extract the parameters of the Δ -resonance even in this case, one has to find an optimum fitting strategy. The discussion of this issue constitutes the main content of this work.

The paper is organized as follows. In section 2 we consider the formalism that is used to calculate the self-energy of the Δ -resonance in the SSE, including a discussion of the infrared regularization procedure in a finite volume. Section 3 is devoted to the numerical calculations and the description of the fitting algorithm and the presentation of our results. In section 4 we introduce analytic parameterizations of the energy spectrum at finite volume, which might be useful for performing fits to the lattice data. Finally, section 5 contains our conclusions.

^{#5}The SSE is a phenomenological extension of chiral perturbation theory in which the nucleon- Δ mass splitting is counted as an additional small parameter. This quantity, however, does not vanish in the chiral limit. The framework of the SSE is laid out in detail in Ref. [30]

2 The formalism

2.1 Extraction of the energy spectrum

Let us consider the two-point function of two Δ -fields, given by Eq. (1), in a Euclidean box and choose the rest frame. After projecting out the spin- $\frac{3}{2}$ state, this two-point function in momentum space develops poles at $p_\mu^n = (iE_n, \mathbf{0})$. In coordinate space, the same two-point function at large Euclidean times t will be given by a sum of exponentials

$$\sum_{\mathbf{x}} \langle 0 | \chi_\mu(x) \bar{\chi}_\nu(0) | 0 \rangle_L \rightarrow \sum_n (z_n)_{\mu\nu} \exp(-E_n t). \quad (2)$$

where the subscript L indicates that the calculations are done at a finite volume $L \times L \times L \times L_t$. We further assume that the size of the box in the time direction L_t is much larger than in the spatial direction L (eventually, $L_t \rightarrow \infty$) Consequently, studying the behavior of this two-point function at large Euclidean times, one is able to extract the energy levels $E_n = E_n(L)$ of the positive parity, spin- $\frac{3}{2}$ states, which are functions of the box size L . In case of a stable Δ -state, finite-size corrections to the lowest energy level vanish exponentially, $E_1(L) - m_\Delta = \exp(-\text{const} \cdot L)$ and in the large- L limit this level yields the value of the stable Δ -mass. This is, however, not the case for the decaying Δ , when the dependence of the energy levels on L is governed by a power rather than by an exponential law. The question is, whether one can extract the parameters of the Δ -resonance from the measured dependence of $E_n(L)$ on L .

2.2 The Lagrangian and Feynman rules

In order to parameterize the volume-dependent energy levels of the system in terms of the Δ -resonance parameters, we calculate the same two-point function in the SSE at finite volume. These calculations are similar to the recent study of the volume-dependent nucleon mass [31–35] – except for the fact that in the present paper we deal with an unstable particle. The calculations are performed by using the effective chiral Lagrangian, which explicitly contains pion, nucleon and Δ degrees of freedom [30, 36] and coincides with the Lagrangian used at infinite volume. The relevant terms (in Minkowski space) are displayed below:

$$\mathcal{L} = \frac{F^2}{4} \langle \partial^\mu U \partial_\mu U^\dagger + \chi^\dagger U + U^\dagger \chi \rangle + \dots + \mathcal{L}_{\pi N} + \mathcal{L}_{\pi \Delta} + \mathcal{L}_{\pi N \Delta}; \quad (3)$$

$$\mathcal{L}_{\pi N} = \mathcal{L}_{\pi N}^{(1)} + \mathcal{L}_{\pi N}^{(2)} + \mathcal{L}_{\pi N}^{(3)} + \dots = \bar{\psi}_N \left\{ \Lambda_{\pi N}^{(1)} + \Lambda_{\pi N}^{(2)} + \Lambda_{\pi N}^{(3)} + \dots \right\} \psi_N,$$

$$\Lambda_{\pi N}^{(1)} = i \not{D} - m_N^0 + \frac{g_A}{2} \not{\psi} \gamma_5,$$

$$\Lambda_{\pi N}^{(2)} = c_1 \langle \chi_+ \rangle - \frac{c_2}{4(m_N^0)^2} \left(\langle u_\mu u_\nu \rangle D^\mu D^\nu + \text{h.c.} \right) + \frac{c_3}{2} \langle u_\mu u^\mu \rangle + \dots,$$

$$\Lambda_{\pi N}^{(3)} = B_1^N \Delta_0 \langle \chi_+ \rangle + B_0^N \Delta_0^3 + \dots; \quad (4)$$

$$\mathcal{L}_{\pi N \Delta} = \mathcal{L}_{\pi N \Delta}^{(1)} + \dots, \quad \mathcal{L}_{\pi N \Delta}^{(1)} = g_{\pi N \Delta} \bar{\psi}_\alpha^i O^{\alpha\beta} w_\beta^i \psi_N + \text{h.c.}; \quad (5)$$

$$\begin{aligned}
\mathcal{L}_{\pi\Delta} &= \mathcal{L}_{\pi\Delta}^{(1)} + \mathcal{L}_{\pi\Delta}^{(2)} + \mathcal{L}_{\pi\Delta}^{(3)} + \dots = -\bar{\psi}_\alpha^i O^{\alpha\mu} \left\{ (\Lambda_{\pi\Delta}^{(1)})_{ij}^{\mu\nu} + (\Lambda_{\pi\Delta}^{(2)})_{ij}^{\mu\nu} + (\Lambda_{\pi\Delta}^{(3)})_{ij}^{\mu\nu} + \dots \right\} O^{\nu\beta} \psi_\beta^j, \\
(\Lambda_{\pi\Delta}^{(1)})_{ij}^{\mu\nu} &= O^{\mu\alpha} \left(g_{\alpha\beta} (i\mathcal{D}_{ij} - \overset{0}{m}_\Delta \xi_{ij}^{3/2}) - \frac{1}{2} \{ \gamma_\alpha \gamma_\beta, (i\mathcal{D}_{ij} - \overset{0}{m}_\Delta \xi_{ij}^{3/2}) \} \right) O^{\beta\nu} + \frac{g_1}{2} \not{x}^{ij} \gamma_5 g^{\mu\nu}, \\
(\Lambda_{\pi\Delta}^{(2)})_{ij}^{\mu\nu} &= g^{\mu\nu} \left\{ a_1 \langle \chi_+ \rangle \delta_{ij} - \frac{a_2}{4(\overset{0}{m}_\Delta)^2} \left(\langle u_\alpha u_\beta \rangle D_{ik}^\alpha D_{kj}^\beta + \text{h.c.} \right) + \frac{a_3}{2} \langle u_\mu u^\mu \rangle \delta_{ij} \right\} + \dots, \\
(\Lambda_{\pi\Delta}^{(3)})_{ij}^{\mu\nu} &= g^{\mu\nu} \delta_{ij} \left\{ B_1^\Delta \Delta_0 \langle \chi_+ \rangle + B_0^\Delta \Delta_0^3 \right\} + \dots, \tag{6}
\end{aligned}$$

where $\langle \dots \rangle$ denotes the trace in flavor space. Throughout, we work in the isospin limit $m_u = m_d = \hat{m}$. The building blocks for the above Lagrangian are defined by

$$\begin{aligned}
U &= u^2, \quad u_\mu = iu^\dagger \partial_\mu U u^\dagger, \quad D_\mu = \partial_\mu + \frac{1}{2} [u^\dagger, \partial_\mu u], \\
\chi &= 2B(s + ip), \quad \chi_+ = u^\dagger \chi u^\dagger + u \chi^\dagger u, \quad s = \hat{m} \mathbf{1} + \dots, \\
w_\mu^i &= \frac{1}{2} \langle \tau^i u_\mu \rangle, \quad D_{ij}^\mu = \delta_{ij} D^\mu - i\epsilon_{ijk} \langle \tau^k D^\mu \rangle, \quad u_{ij}^\mu = \delta_{ij} u^\mu \tag{7}
\end{aligned}$$

and

$$O^{\mu\nu} = g^{\mu\nu} - \frac{2}{d} \gamma^\mu \gamma^\nu. \tag{8}$$

In these formulae, $U = \exp\{i\boldsymbol{\tau} \cdot \boldsymbol{\pi}/F\}$, ψ_N and ψ_μ^i represent the pion, nucleon and Δ interpolating fields, respectively. Further, $\overset{0}{m}_N$, $\overset{0}{m}_\Delta$ are the masses of the nucleon and the Δ in the chiral limit, and $\Delta_0 = \overset{0}{m}_\Delta - \overset{0}{m}_N$ is the Δ -nucleon mass difference in this limit. The pion mass is given by $M_\pi^2 = 2B\hat{m} + O(\hat{m}^2)$. Furthermore, F , g_A , $g_{\pi N\Delta}$ denote the pion decay constant, the nucleon axial-vector constant and the $\pi N\Delta$ coupling constant in the chiral limit and $c_i, B_i^N, a_i, B_i^\Delta$ denote various low-energy constants (LECs). Finally, the projectors onto the isospin- $\frac{3}{2}$ and isospin- $\frac{1}{2}$ subspaces are defined by

$$\xi_{ij}^{3/2} = \delta_{ij} - \frac{1}{3} \tau_i \tau_j, \quad \xi_{ij}^{1/2} = \frac{1}{3} \tau_i \tau_j, \quad \xi_{ij}^{3/2} + \xi_{ij}^{1/2} = \delta_{ij}. \tag{9}$$

The free Δ -propagator in d -dimensional space can be read off from the quadratic part of the Lagrangian

$$i\langle 0 | T \psi_\mu^{0,i}(x) \bar{\psi}_\nu^{0,j}(0) | 0 \rangle = \int \frac{d^d p}{(2\pi)^d} e^{-ipx} S_{\mu\nu}^0(p) \xi^{3/2,ij} \tag{10}$$

with

$$\Sigma^L = \frac{\pi}{\Delta} + \frac{\pi}{\mathbf{N}} + \frac{\mathbf{a}_1, \mathbf{B}_0^\Delta, \mathbf{B}_1^\Delta}{\times}$$

Figure 2: The self-energy of the Δ at $O(\epsilon^3)$ in the SSE.

where the projectors onto the spin- $\frac{3}{2}$ and spin- $\frac{1}{2}$ states are defined as

$$\begin{aligned} (P^{3/2})_{\mu\nu} &= g_{\mu\nu} - \frac{1}{d-1} \gamma_\mu \gamma_\nu - \frac{1}{(d-1)p^2} (\not{p} \gamma_\mu p_\nu + p_\mu \gamma_\nu \not{p}) - \frac{d-4}{d-1} \frac{p_\mu p_\nu}{p^2}, \\ (P_{12}^{1/2})_{\mu\nu} &= \frac{1}{\sqrt{d-1} p^2} (p_\mu p_\nu - \not{p} p_\nu \gamma_\mu), \\ (P_{21}^{1/2})_{\mu\nu} &= \frac{1}{\sqrt{d-1} p^2} (\not{p} p_\mu \gamma_\nu - p_\mu p_\nu), \\ (P_{22}^{1/2})_{\mu\nu} &= \frac{p_\mu p_\nu}{p^2}, \\ (P_{11}^{1/2})_{\mu\nu} &= g_{\mu\nu} - (P^{3/2})_{\mu\nu} - (P_{22}^{1/2})_{\mu\nu}. \end{aligned} \quad (12)$$

These projectors obey the following relations

$$\begin{aligned} (P_{ij}^{1/2})_{\mu\lambda} (P_{kl}^{1/2})^{\lambda\nu} &= \delta_{jk} (P_{il}^{1/2})_\mu^\nu, \\ (P^{3/2})_{\mu\lambda} (P_{ij}^{1/2})^{\lambda\nu} &= (P_{ij}^{1/2})_{\mu\lambda} (P^{3/2})^{\lambda\nu} = 0, \\ (P^{3/2})_{\mu\lambda} (P^{3/2})^{\lambda\nu} &= (P^{3/2})_\mu^\nu, \quad i, j, k, l = 1, 2. \end{aligned} \quad (13)$$

2.3 The poles of the propagator

The Δ propagator after inclusion of the self-energy diagrams (see Fig. 2) becomes

$$i \langle 0 | T \psi_\mu^i(x) \bar{\psi}_\nu^j(0) | 0 \rangle = \int \frac{d^d p}{(2\pi)^d} e^{-ipx} S_{\mu\nu}^L(p) \xi^{3/2, ij} \quad (14)$$

where

$$S_{\mu\nu}^L(p) = -\frac{1}{\overset{0}{m}_\Delta - \not{p} + \Sigma^L(p)} (P^{3/2})_{\mu\nu} + \dots, \quad \Sigma^L(p) = \not{p} \Sigma_1^L(p^2) + \overset{0}{m}_\Delta \Sigma_2^L(p^2), \quad (15)$$

and the ellipses stand for the terms with spin- $\frac{1}{2}$ projectors. The poles of the propagator are given by the zeros of the denominator

$$\overset{0}{m}_\Delta - \not{p} + \not{p} \Sigma_1^L(p^2) + \overset{0}{m}_\Delta \Sigma_2^L(p^2) = 0. \quad (16)$$

We further introduce the quantities

$$\tilde{\Sigma}_i^L(p^2) = \Sigma_i^L(p^2) - \text{Re} \Sigma_i(p^2), \quad i = 1, 2, \quad (17)$$

where $\Sigma(p) = \not{p}\Sigma_1(p^2) + \overset{0}{m}_\Delta \Sigma_2(p^2)$ denotes the self-energy part of the Δ -resonance, calculated in the infinite volume (note that this quantity is complex below the decay threshold). Introducing now the physical Δ -mass (the real part of the pole mass) through the conventional definition (in the infinite volume)

$$m_\Delta = \overset{0}{m}_\Delta (1 + \text{Re } \Sigma_1(m_\Delta^2) + \text{Re } \Sigma_2(m_\Delta^2)) + O(p^4), \quad (18)$$

it can be seen that, at the order we are working, Eq. (16) can be rewritten by using the physical mass instead of the mass in the chiral limit

$$m_\Delta - \not{p} + \not{p}\tilde{\Sigma}_1^L(p^2) + m_\Delta\tilde{\Sigma}_2^L(p^2) = 0. \quad (19)$$

Performing the analytic continuation to Euclidian space $p_\mu = (p_0, \mathbf{p}) = (i\hat{p}_4, \hat{\mathbf{p}})$ and choosing the center-of-mass frame $\hat{p}_\mu = (\omega, \mathbf{0})$, from Eq. (19) we finally get

$$m_\Delta^2(1 + \tilde{\Sigma}_2^L(-\omega^2))^2 + \omega^2(1 - \tilde{\Sigma}_1^L(-\omega^2))^2 = 0. \quad (20)$$

2.4 Calculation of the self-energy at $O(\epsilon^3)$

Only pion-nucleon and pion- Δ loops, which are shown in Fig. 2, contribute to the quantities $\tilde{\Sigma}_i^L(-\omega^2)$. The counterterm contribution is independent on L and thus drops out from the final expression. One obtains

$$\tilde{\Sigma}_i^L(-\omega^2) = \tilde{\Sigma}_{i,N}^L(-\omega^2) + \tilde{\Sigma}_{i,\Delta}^L(-\omega^2), \quad i = 1, 2, \quad (21)$$

where

$$\tilde{\Sigma}_{1,N}^L(-\omega^2) = \frac{g_{\pi N\Delta}^2}{F^2} \left\{ \tilde{W}_2^N(-\omega^2) - \tilde{W}_3^N(-\omega^2) \right\}, \quad \tilde{\Sigma}_{2,N}^L(-\omega^2) = \frac{g_{\pi N\Delta}^2}{F^2} \frac{m_N}{m_\Delta} \tilde{W}_2^N(-\omega^2) \quad (22)$$

and

$$\begin{aligned} \tilde{\Sigma}_{1,\Delta}^L(-\omega^2) &= \frac{5g_1^2}{12F^2} \left\{ -\tilde{T}_0^\pi + (m_\Delta^2 + \omega^2)\tilde{W}_0^\Delta(-\omega^2) + (m_\Delta^2 - \omega^2)\tilde{W}_1^\Delta(-\omega^2) \right. \\ &\quad \left. - \frac{2}{3m_\Delta^2} (3m_\Delta^2 + \omega^2)\tilde{W}_2^\Delta(-\omega^2) - \frac{2}{3m_\Delta^2} (m_\Delta^2 - \omega^2)\tilde{W}_3^\Delta(-\omega^2) \right\}, \\ \tilde{\Sigma}_{2,\Delta}^L(-\omega^2) &= \frac{5g_1^2}{12F^2} \left\{ -\tilde{T}_0^\pi + (m_\Delta^2 + \omega^2)\tilde{W}_0^\Delta(-\omega^2) - 2\omega^2\tilde{W}_1^\Delta(-\omega^2) \right. \\ &\quad \left. - \frac{4}{3}\tilde{W}_2^\Delta(-\omega^2) + \frac{4\omega^2}{3m_\Delta^2}\tilde{W}_3^\Delta(-\omega^2) \right\}. \end{aligned} \quad (23)$$

In the above expressions, the quantity \tilde{T}_0^π corresponds to the pion tadpole and $\tilde{W}_i^N(-\omega^2)$, $\tilde{W}_i^\Delta(-\omega^2)$ to the πN and $\pi\Delta$ scalar loop functions, respectively (note that the tadpoles emerge from the one-loop diagrams shown in Fig. 2 after simplifying the numerators). An exact definition of these quantities is given below. Further, in these expressions one may take $d = 4$ because all ultraviolet divergences are contained in the infinite-volume integrals which, at the end, are included in the definition of the infinite-volume mass m_Δ . Further, at the order we are working, the quantity F can be replaced by the pion decay constant F_π . At the end, the self-energy part in a finite volume at $O(\epsilon^3)$ is expressed in terms of physical quantities only.

In the calculations at finite volume the loop integrals are replaced by infinite sums over discrete lattice momenta $\mathbf{k}_n = 2\pi\mathbf{n}/L$, $\mathbf{n} \in Z^3$ in spatial dimensions (see, e.g. [37]). To ease the notation, below we give the loop functions with the infinite-volume part included. In order to arrive at the quantities that enter Eqs. (22,23), one has first to isolate the infinite-volume part and then subtract it, e.g.

$$\tilde{T}_0^\pi = T_0^\pi - T_0^\pi|_{L \rightarrow \infty}. \quad (24)$$

Consequently, the expressions that are given below, are ultraviolet divergent and imply the application of some kind of regularization. Here we do not refer to a particular regularization procedure explicitly, since the divergent infinite-volume part will be always subtracted before the actual calculations are performed.

The one-loop integrals that contribute to the self-energy of the Δ -resonance, are listed below ($X = N, \Delta$). These are tadpole diagrams

$$\begin{aligned} T_0^\pi &= \int_{-\infty}^{\infty} \frac{dk_4}{2\pi} \frac{1}{L^3} \sum_{\mathbf{n}} \frac{1}{M_\pi^2 + k_n^2}, \\ T_0^X &= \int_{-\infty}^{\infty} \frac{dk_4}{2\pi} \frac{1}{L^3} \sum_{\mathbf{n}} \frac{1}{m_X^2 + k_n^2}, \\ \left(\delta_{\alpha\beta} - \frac{\hat{p}_\alpha \hat{p}_\beta}{\hat{p}^2} \right) N_2^\pi + \frac{\hat{p}_\alpha \hat{p}_\beta}{\hat{p}^2} T_2^\pi &= - \int_{-\infty}^{\infty} \frac{dk_4}{2\pi} \frac{1}{L^3} \sum_{\mathbf{n}} \frac{k_\alpha k_\beta}{M_\pi^2 + k_n^2}, \\ \left(\delta_{\alpha\beta} - \frac{\hat{p}_\alpha \hat{p}_\beta}{\hat{p}^2} \right) N_2^X + \frac{\hat{p}_\alpha \hat{p}_\beta}{\hat{p}^2} T_2^X &= - \int_{-\infty}^{\infty} \frac{dk_4}{2\pi} \frac{1}{L^3} \sum_{\mathbf{n}} \frac{k_\alpha k_\beta}{m_X^2 + k_n^2}, \end{aligned} \quad (25)$$

as well as the meson-baryon loop functions

$$\begin{aligned} W_0^X(-\omega^2) &= \int_{-\infty}^{\infty} \frac{dk_4}{2\pi} \frac{1}{L^3} \sum_{\mathbf{n}} \frac{1}{(M_\pi^2 + k_n^2)(m_X^2 + (\hat{p} - k_n)^2)}, \\ \hat{p}_\alpha W_1^X(-\omega^2) &= \int_{-\infty}^{\infty} \frac{dk_4}{2\pi} \frac{1}{L^3} \sum_{\mathbf{n}} \frac{k_\alpha}{(M_\pi^2 + k_n^2)(m_X^2 + (\hat{p} - k_n)^2)}, \\ \left(\delta_{\alpha\beta} - \frac{\hat{p}_\alpha \hat{p}_\beta}{\hat{p}^2} \right) W_2^X(-\omega^2) + \frac{\hat{p}_\alpha \hat{p}_\beta}{\hat{p}^2} S_2^X(-\omega^2) &= - \int_{-\infty}^{\infty} \frac{dk_4}{2\pi} \frac{1}{L^3} \sum_{\mathbf{n}} \frac{k_\alpha k_\beta}{(M_\pi^2 + k_n^2)(m_X^2 + (\hat{p} - k_n)^2)}, \\ (\delta_{\alpha\beta} \hat{p}_\sigma + \delta_{\sigma\alpha} \hat{p}_\beta + \delta_{\beta\sigma} \hat{p}_\alpha) W_3^X(-\omega^2) + \frac{\hat{p}_\alpha \hat{p}_\beta \hat{p}_\sigma}{\hat{p}^2} S_3^X(-\omega^2) &= - \int_{-\infty}^{\infty} \frac{dk_4}{2\pi} \frac{1}{L^3} \sum_{\mathbf{n}} \frac{k_\alpha k_\beta k_\sigma}{(M_\pi^2 + k_n^2)(m_X^2 + (\hat{p} - k_n)^2)}, \end{aligned} \quad (26)$$

with the Euclidean 4-momentum $(k_n)_\mu = (k_4, \mathbf{k}_n)$. After subtracting the infinite-volume piece, the following recurrence relations between various functions can be obtained:

$$\begin{aligned} \tilde{N}_2^\pi &= \frac{1}{3} (M_\pi^2 \tilde{T}_0^\pi - \tilde{T}_2^\pi), \quad \tilde{N}_2^X = \frac{1}{3} (m_X^2 \tilde{T}_0^X - \tilde{T}_2^X), \\ \tilde{W}_1^X(-\omega^2) &= \frac{\omega^2 + m_X^2 - M_\pi^2}{2\omega^2} \tilde{W}_0^X(-\omega^2) - \frac{\tilde{T}_0^\pi}{2\omega^2} + \frac{\tilde{T}_0^X}{2\omega^2}, \\ \tilde{W}_2^X(-\omega^2) &= \frac{1}{12\omega^2} \left\{ \lambda(-\omega^2, m_X^2, M_\pi^2) \tilde{W}_0^X(-\omega^2) - (\omega^2 + m_X^2 - M_\pi^2) \tilde{T}_0^\pi - (\omega^2 - m_X^2 + M_\pi^2) \tilde{T}_0^X \right\}, \end{aligned}$$

$$\tilde{W}_3^X(-\omega^2) = \frac{\omega^2 + m_X^2 - M_\pi^2}{2\omega^2} \tilde{W}_2^X(-\omega^2) - \frac{1}{6\omega^2} \left\{ M_\pi^2 \tilde{T}_0^\pi - \tilde{T}_2^\pi - m_X^2 \tilde{T}_0^X + \tilde{T}_2^X \right\}, \quad (27)$$

where $\lambda(x, y, z) = x^2 + y^2 + z^2 - 2xy - 2yz + 2zx$ denotes the usual triangle function.

2.5 Calculation of the scalar integrals

The calculation of the tadpole graphs is straightforward and is carried out by using standard techniques (see, e.g. [33, 34]). We demonstrate the method for the case of the pion tadpole. Using dimensional regularization to tame the ultraviolet divergence in Eq. (25), one gets

$$\begin{aligned} T_0^\pi &= \frac{1}{L^3} \int_{-\infty}^{\infty} \frac{dk_4}{2\pi} \int d^{d-1}\mathbf{k} \frac{1}{M_\pi^2 + k_4^2 + \mathbf{k}^2} \sum_{\mathbf{n}} \delta^{d-1}\left(\mathbf{k} - \frac{2\pi\mathbf{n}}{L}\right) \\ &= \int \frac{d^d k}{(2\pi)^d} \frac{1}{M_\pi^2 + k_4^2 + \mathbf{k}^2} \sum_{\mathbf{j}} e^{iL\mathbf{k}\mathbf{j}}, \end{aligned} \quad (28)$$

where the Poisson formula

$$\sum_{n=-\infty}^{+\infty} \delta(x - n) = \sum_{n=-\infty}^{+\infty} e^{2\pi i n x} \quad (29)$$

has been used to arrive at the second equality. Further, in this sum the term with $\mathbf{j} = 0$ corresponds to the infinite-volume integral. Separating this term, we finally obtain

$$\begin{aligned} T_0^\pi &= \int \frac{d^d k}{(2\pi)^d} \frac{1}{M_\pi^2 + k_4^2 + \mathbf{k}^2} + \sum_{j \neq 0} \frac{1}{4\pi^2 L j} \int_0^\infty dk_4 e^{-Lj \sqrt{M_\pi^2 + k_4^2}} \\ &= T_0^\pi \Big|_{L \rightarrow \infty} + \frac{M_\pi^2}{4\pi^2} \sum_{j \neq 0} \frac{K_1(M_\pi L j)}{M_\pi L j}, \end{aligned} \quad (30)$$

where $j = |\mathbf{j}| = \sqrt{j_1^2 + j_2^2 + j_3^2}$ and $K_\nu(z)$ denotes the modified Bessel function.

The final result for the tadpoles is given by

$$\begin{aligned} \tilde{T}_0^\pi &= \frac{M_\pi^2}{4\pi^2} \sum_{\mathbf{j} \neq 0} \frac{K_1(M_\pi L j)}{M_\pi L j}, \quad \tilde{T}_0^X = \frac{m_X^2}{4\pi^2} \sum_{\mathbf{j} \neq 0} \frac{K_1(m_X L j)}{m_X L j}, \\ \tilde{T}_2^\pi &= -\frac{M_\pi^4}{4\pi^2} \sum_{\mathbf{j} \neq 0} \frac{K_2(M_\pi L j)}{(M_\pi L j)^2}, \quad \tilde{T}_2^X = -\frac{m_X^4}{4\pi^2} \sum_{\mathbf{j} \neq 0} \frac{K_2(m_X L j)}{(m_X L j)^2}. \end{aligned} \quad (31)$$

In the calculation of the meson-baryon loop functions one has to distinguish between two cases. In the $\pi\Delta$ loop, the variable $-\omega^2$ is below threshold. Using the Feynman parameterization, one may combine two denominators and then use the same technique as for the calculation of the tadpole contribution. As a result, one gets

$$\begin{aligned} \tilde{W}_0^\Delta(-\omega^2) &= \frac{1}{8\pi^2} \int_0^1 dx \sum_{\mathbf{j} \neq 0} K_0\left(Lj \sqrt{g_\Delta(x, -\omega^2)}\right), \\ g_\Delta(x, -\omega^2) &= (1-x)M_\pi^2 + xm_\Delta^2 + x(1-x)\omega^2. \end{aligned} \quad (32)$$

Note that for $-\omega^2$ close to m_Δ^2 the function $g_\Delta(x, -\omega^2)$ never vanishes in the integration region.

In contrast to the above example, the πN loop can not be calculated by using the same method, because the variable $-\omega^2$ can now be above the decay threshold $\Delta \rightarrow N\pi$. To calculate this quantity, the following trick has been used. First, in order to avoid the ultraviolet divergence in the infinite sum over momenta, we have subtracted the integral at some scale $\omega^2 = \mu^2$ below threshold (one subtraction is enough for the convergence, but double subtraction enables one to achieve faster convergence). Now in the subtraction terms one is allowed to use the same technique as in the calculation of the $\pi\Delta$ loop, because $-\mu^2$ is below threshold. This strategy is illustrated below in detail. The quantity $\tilde{W}_0^N(-\omega^2)$ which we are looking for is split into several terms

$$\begin{aligned}
\tilde{W}_0^N(-\omega^2) &= W_0^N(-\omega^2) - \text{Re} W_0^N(-\omega^2) \Big|_{L \rightarrow \infty} = H_1(-\omega^2) + H_2(-\omega^2) + H_3(-\omega^2), \\
H_1(-\omega^2) &= \left\{ W_0^N(-\omega^2) - W_0^N(-\mu^2) + (\omega^2 - \mu^2) \frac{d}{d\omega^2} W_0^N(-\omega^2) \Big|_{\omega^2 = \mu^2} \right\}, \\
H_2(-\omega^2) &= \left\{ \tilde{W}_0^N(-\mu^2) + (\omega^2 - \mu^2) \frac{d}{d\omega^2} \tilde{W}_0^N(-\omega^2) \Big|_{\omega^2 = \mu^2} \right\}, \\
H_3(-\omega^2) &= - \left\{ \text{Re} W_0^N(-\omega^2) - W_0^N(-\mu^2) + (\omega^2 - \mu^2) \frac{d}{d\omega^2} W_0^N(-\omega^2) \Big|_{\omega^2 = \mu^2} \right\} \Big|_{L \rightarrow \infty}. \quad (33)
\end{aligned}$$

The first term is the twice-subtracted infinite momentum sum, where the integration over k_4 is explicitly performed

$$\begin{aligned}
H_1(-\omega^2) &= (\omega^2 - \mu^2)^2 \frac{1}{L^3} \sum_{\mathbf{n}} \frac{E_N + E_\pi}{2E_N E_\pi} \frac{1}{\omega^2 + (E_N + E_\pi)^2} \frac{1}{(\mu^2 + (E_N + E_\pi)^2)^2}, \\
E_N &= \sqrt{m_N^2 + \mathbf{k}_n^2}, \quad E_\pi = \sqrt{M_\pi^2 + \mathbf{k}_n^2}. \quad (34)
\end{aligned}$$

The second expression corresponds to the subtraction term

$$\begin{aligned}
H_2(-\omega^2) &= \frac{1}{8\pi^2} \int_0^1 dx \sum_{\mathbf{j} \neq 0} \left(K_0 \left(Lj \sqrt{g_N(x, -\mu^2)} \right) \right. \\
&\quad \left. - (\omega^2 - \mu^2) \frac{x(1-x)Lj}{2\sqrt{g_N(x, -\mu^2)}} K_1 \left(Lj \sqrt{g_N(x, -\mu^2)} \right) \right), \\
g_N(x, -\mu^2) &= (1-x)M_\pi^2 + xm_N^2 + x(1-x)\mu^2. \quad (35)
\end{aligned}$$

Furthermore, the remainder is included into the third term, which contains only quantities evaluated in the infinite volume

$$\begin{aligned}
H_3(-\omega^2) &= -\frac{B_\omega}{32\pi^2\omega^2} \left\{ \ln \frac{-\omega^2 + m_N^2 - M_\pi^2 + B_\omega}{-\omega^2 + m_N^2 - M_\pi^2 - B_\omega} + \ln \frac{-\omega^2 - m_N^2 + M_\pi^2 + B_\omega}{-\omega^2 - m_N^2 + M_\pi^2 - B_\omega} \right\} \\
&+ \frac{B_\mu}{16\pi^2\mu^2} \left\{ \arctan \frac{-\mu^2 + m_N^2 - M_\pi^2}{B_\mu} + \arctan \frac{-\mu^2 - m_N^2 + M_\pi^2}{B_\mu} \right\} \\
&- \frac{\omega^2 - \mu^2}{16\pi^2\mu^2} \left\{ 1 + \frac{(\omega^2 - \mu^2)(m_N^2 - M_\pi^2)}{2\omega^2\mu^2} \ln \frac{m_N^2}{M_\pi^2} - \frac{\mu^2(m_N^2 + M_\pi^2) + (m_N^2 - M_\pi^2)^2}{\mu^2 B_\mu} \right. \\
&\times \left. \left(\arctan \frac{-\mu^2 + m_N^2 - M_\pi^2}{B_\mu} + \arctan \frac{-\mu^2 - m_N^2 + M_\pi^2}{B_\mu} \right) \right\}, \\
B_\omega &= \lambda^{1/2}(-\omega^2, m_N^2, M_\pi^2), \quad B_\mu = \lambda^{1/2}(-\mu^2, m_N^2, M_\pi^2). \quad (36)
\end{aligned}$$

2.6 Remarks

- a) In order to study baryon resonances, the volume should be taken much larger than in the case of stable particles since for excited states, the volume-dependent effects decrease only as powers of L and not by an exponential law as for stable particles. More precisely, the parameter L should be large enough, so that one could neglect all contributions of the type $\exp(-\text{const} \cdot M_\pi L)$ (see, e.g. [37,38]) as compared to the corrections that decrease according to the power law.
- b) The Lagrangians, given by Eqs. (3,4,5) and Eq. (6) do not contain the so-called “off-shell” pieces that do not contribute to observable quantities like the S -matrix elements or transition currents. They could in principle contribute to the self-energy of the Δ , which is not an “on-shell” quantity. However, eliminating these terms at the diagrammatic level corresponds to canceling one of the propagators in the loop. The pertinent diagram turns into a tadpole, which vanishes exponentially. Therefore, for large values of L , where the exponential factors can be neglected, the off-shell couplings do not contribute to the self-energy.
- c) The same line of reasoning can be used to show that the contribution from the spin- $\frac{1}{2}$ components of the Δ -propagator is irrelevant at finite volume.
- d) As seen from Eq. (32), the whole L -dependent part of the contribution from the $\pi\Delta$ loop is exponentially suppressed at large L . The same is true for all tadpoles. Even if we have retained them in the final expressions for completeness, the L -dependent part thereof can be safely neglected at any stage of the calculation. Indeed, we have checked numerically that the contribution from the $\pi\Delta$ loop is very small and does not affect the results.
- e) Covariant SSE calculations in the baryon sector at an infinite volume are performed by e.g. using infrared regularization (IR), which leads to a consistent power counting in the presence of the (large) baryon mass. This method has been also applied in the calculations at finite volume (see, e.g. [33]). The procedure, adopted in that work, amounts to merely extending the integration interval over the pertinent Feynman parameter from $[0, 1]$ to $[0, \infty[$, in a complete analogy to what is done at an infinite volume. In other words, in the context of the present problem it is equivalent to setting the N and Δ tadpoles to 0 in Eq. (31) and to extending the integration over dx in Eq. (32) from 0 to ∞ . It is, however, not immediately clear how this procedure can be generalized to the case when $-\omega^2$ is above threshold, see Eqs. (33,34,35,36). Our method is different from the one described above. Namely, we note first that applying IR in an infinite volume is equivalent to using ordinary dimensional regularization and changing the renormalization prescription. Next, going to a finite volume implies using the same Lagrangian, while replacing integrals by sums in the loops. In other words, our prescription reduces to using IR only in the infinite-volume self-energy $\Sigma(p)$, whereas in the finite-volume piece $\tilde{\Sigma}^L(p) = \Sigma^L(p) - \Sigma(p)$ ordinary dimensional regularization has been used. It is clear that in our case, unlike Ref. [33], the counterterms, corresponding to the above-mentioned additional renormalization, are L -independent.

In the case of a stable particle changing the prescription from one to another amounts to introducing corrections which vanish as $\exp(-\text{const} \cdot m_X L)$ with $X = N, \Delta$ at large L . This happens, in particular, for the volume-dependent nucleon mass, considered in Ref. [33]. It is clear that in this case the difference between the two prescriptions is physically irrelevant. It remains to be seen, what kind of statement can be made in case of an unstable particle.

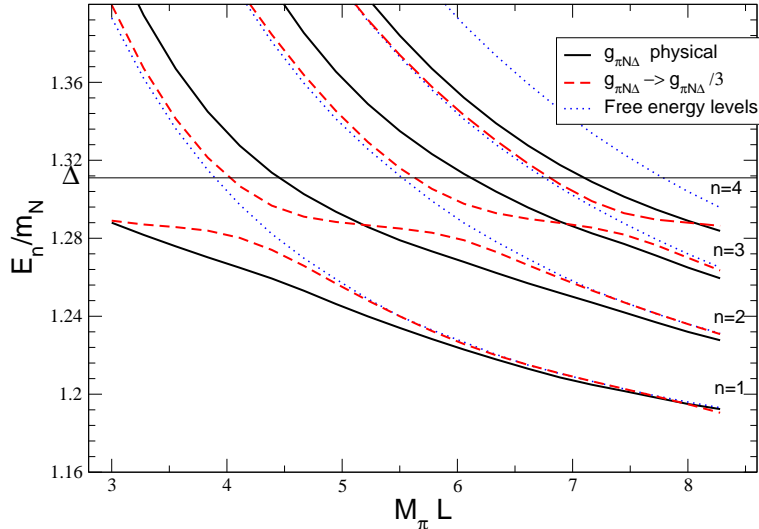


Figure 3: The dependence of the energy levels in a finite box on the box size L for different values of the coupling constant $g_{\pi N\Delta}$. The avoided level crossing, which is clearly seen at small values of $g_{\pi N\Delta}$ (dashed lines), is washed out for the physical value of this coupling constant (solid lines). For comparison, we also display the free energy levels (dotted lines). It is seen that the energy levels in the presence of the interaction interpolate between different free energy levels. As expected, an abrupt change emerges in the vicinity of the resonance energy (the resonance position corresponds to the solid horizontal line).

3 Numerical results

Solving Eq. (20) for different values of L numerically we get the dependence of the energy levels $E_n(L)$ of the system, placed in a Euclidean box of size L . At this order, the energy levels depend on two parameters, namely the mass m_Δ and the coupling constant $g_{\pi N\Delta}$. The term containing the coupling constant g_1 is exponentially suppressed and we assume that m_N, M_π, F_π are determined independently in the same lattice calculations. We wish to investigate whether one can determine m_Δ and $g_{\pi N\Delta}$ at a reasonable accuracy from a fit to the energy levels.

The results of calculations of the energy levels for the physical values of all parameters are shown in Fig. 3 (solid lines). We use the following values for the particle masses: $M_\pi = 140$ MeV, $m_N = 940$ MeV and $m_\Delta = 1210$ MeV (the real part of the pole mass) and for the pion decay constant $F_\pi = 92.4$ MeV. Further, we fix the physical value of the $\pi N\Delta$ coupling constant as $g_{\pi N\Delta} = 1.2$ (at $M_\pi = 140$ MeV). This corresponds to the value $g_\Delta^2/4\pi = 13.5$ GeV $^{-2}$ ($g_{\pi N\Delta} = F_\pi g_\Delta$) obtained by using the pole approximation in dispersion relations, see Ref. [39]. Finally, we take $g_1 = 2.0$ from Ref. [36] (nothing changes if we take $g_1 = 0$). As we see, the coupling of the Δ to the πN -system is so strong that the nice structure with the avoided level crossing has been almost completely washed out. It will resurface again, if the input value of $g_{\pi N\Delta}$ is drastically reduced by hand (dashed lines in the same figure). This property, however, can not be meaningfully used in the fitting procedure. It is clear that, in order to perform the fit, another strategy, not linked to the identification of the resonance energy from the position of the avoided level crossing, should be looked for.

In order to find such a strategy, we continue to study the structure of the energy levels, as well as the dependence on all available parameters. In particular, we start with varying m_Δ keeping all other parameters fixed. Consider for instance the lowest energy level shown in Fig. 4, where the dependence

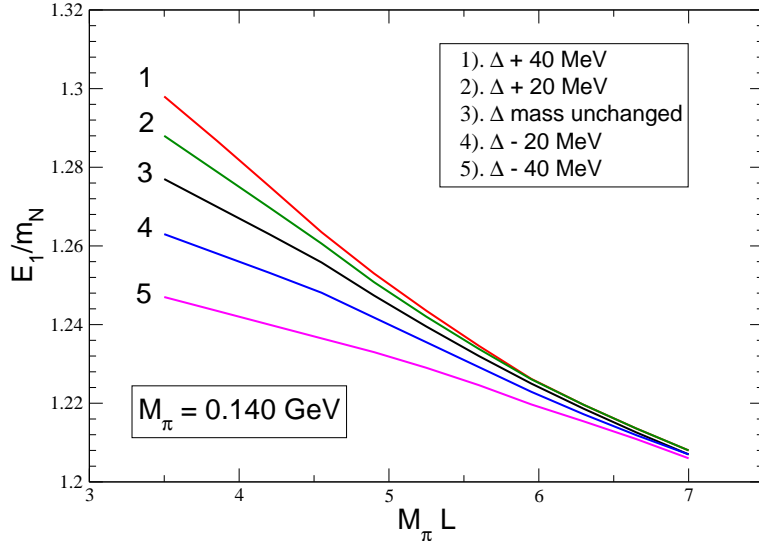


Figure 4: The lowest energy level for different input values of m_Δ and the physical values of $g_{\pi N\Delta}$ and M_π .

of the energy eigenvalue on L is plotted for different input value of m_Δ . It is seen that the curves are almost linear in the variable $\hat{L} = M_\pi L$ from the interval shown, with the tangent that monotonically decreases with decreasing m_Δ . This property can be used for extracting m_Δ . More precisely, one has to measure E_1 on the lattice for different \hat{L} and fit the curve, treating m_Δ as a free parameter. The lattice data decide which of the curves in Fig. 6 has to be chosen. Since each curve corresponds to a particular value of the m_Δ , the fit to the lowest level determines this parameter unambiguously (provided $g_{\pi N\Delta}$ is known).

Next, we consider the possibility of the determination of the $\pi N\Delta$ coupling constant. To this end, one has to find a quantity that could be maximally sensitive to $g_{\pi N\Delta}$ and try to extract this coupling by a fitting procedure. Bearing in mind the level structure in the presence of a very narrow resonance (avoided level crossing), we expect that the difference of two energy levels $E_2(L) - E_1(L)$ can strongly depend on the width of the resonance. In Fig. 5 we plot the quantity $E_2(L) - E_1(L)$ against the variable \hat{L} at a fixed value of m_Δ and varying the parameter $g_{\pi N\Delta}$. The avoided level crossing in this quantity – at small values of the parameter $g_{\pi N\Delta}$ – is seen as a sharp minimum near the value of \hat{L} where the crossing takes place and the value of the function at the minimum determines the width. As evident from Fig. 5, even at the physical value of $g_{\pi N\Delta}$ one may observe a remnant of the avoided level crossing – a plateau, which disappears if $g_{\pi N\Delta}$ increases further. Given a rather pronounced dependence of the quantities plotted in Fig. 5 on the input value of $g_{\pi N\Delta}$, one may expect that fitting would allow one to determine this coupling constant with a reasonable accuracy.

We are now in a position to describe our proposal for determining the parameters of the Δ -resonance m_Δ and $g_{\pi N\Delta}$ from the lattice data, which is expected to work, even if the width of the resonance is not very small. In brief, we propose to fit the first few energy levels, measured on the lattice, to the calculated energy levels, which are parameterized by the free parameters m_Δ and $g_{\pi N\Delta}$. Further, it could be advantageous to carry out this procedure iteratively. Fix first the decay constant to some input value and determine the Δ -mass from the \hat{L} -dependence of the lowest energy level, see Fig. 4. With the newly determined Δ -mass plot the difference $E_2(L) - E_1(L)$ and fit the parameter $g_{\pi N\Delta}$ to the data, see Fig. 5. Repeat the procedure until convergence is achieved.

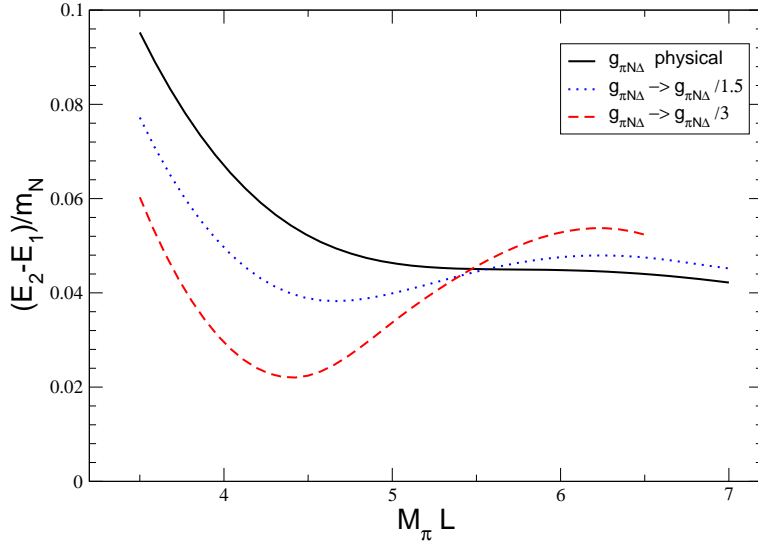


Figure 5: The difference of the first two energy levels for different values of $g_{\pi N\Delta}$ and the physical value of M_π . For small values of the coupling constant there is a dip, corresponding to the avoided level crossing. A plateau is clearly visible even for the physical value of $g_{\pi N\Delta}$.

Finally, we wish to comment on the dependence of the energy levels on the other parameter which is at our disposal, namely the quark (pion) mass. Since this structure depends only on the physical nucleon and Δ masses, in the present (exploratory) study of the problem we have restricted ourselves to the $O(\epsilon^2)$ expressions of the baryon masses

$$m_N = m_N^{\text{phys}} - 4c_1(M_\pi^2 - (M_\pi^{\text{phys}})^2), \quad m_\Delta = m_\Delta^{\text{phys}} - 4a_1(M_\pi^2 - (M_\pi^{\text{phys}})^2) \quad (37)$$

and take $c_1 = -0.9 \text{ GeV}^{-1}$, $a_1 = -0.3 \text{ GeV}^{-1}$ [36] (note that c_1 and a_1 enter only through the nucleon and Δ masses in the infinite volume, so the choice of particular numerical values for these constants does not affect our conclusions). Moreover, we neglect the pion mass dependence of the coupling constant F_π , since the pertinent correction arises at higher order. The above simple case perfectly models the real situation: the mass difference between m_Δ and $m_N + M_\pi$ monotonically decreases with the increase of M_π and vanishes at around $M_\pi = 210 \text{ MeV}$. Below threshold, the structure of the energy levels and the dependence on the parameters m_Δ , $g_{\pi N\Delta}$ is similar to the case with $M_\pi = 140 \text{ MeV}$. After crossing the threshold from below, the Δ is stable and one expects that the finite-volume corrections to the lowest energy level get exponentially suppressed.

Fig. 6 clearly illustrates this pattern. In this figure, the lowest-order energy level is plotted at three different values of the pion mass and the physical value of the decay constant. As we see, the curve is rather smooth in all cases and monotonically flattens as the decay threshold is approached from below. This property can be discussed in a more quantitative fashion. Namely, fitting the level energy in Fig. 6 $\hat{E}_1 = E_1/m_N$ to the variable \hat{L} within the interval $3 \leq \hat{L} \leq 8.3$ with a linear function $\hat{E}_1 = A + B\hat{L}$, for the different values of the mass gap $\omega_0 = m_\Delta - m_N - M_\pi$ we get: $(A, B) = (1.34, -0.019)$ for $\omega_0 = 130 \text{ MeV}$, $(A, B) = (1.30, -0.009)$ for $\omega_0 = 78 \text{ MeV}$, $(A, B) = (1.25, -0.006)$ for $\omega_0 = 20 \text{ MeV}$. It is seen that, while the parameter A remains almost stable, the linear coefficient decreases monotonically. It is important to observe that there is no sign of irregularity in the quantity $E_1(L)$, when one crosses the threshold. Finally, we would like to mention that here the distance at which the chiral extrapolation takes place is not bound from below and could be taken smaller than the distance to the decay threshold. Consequently, the extrapolation error could be reduced.

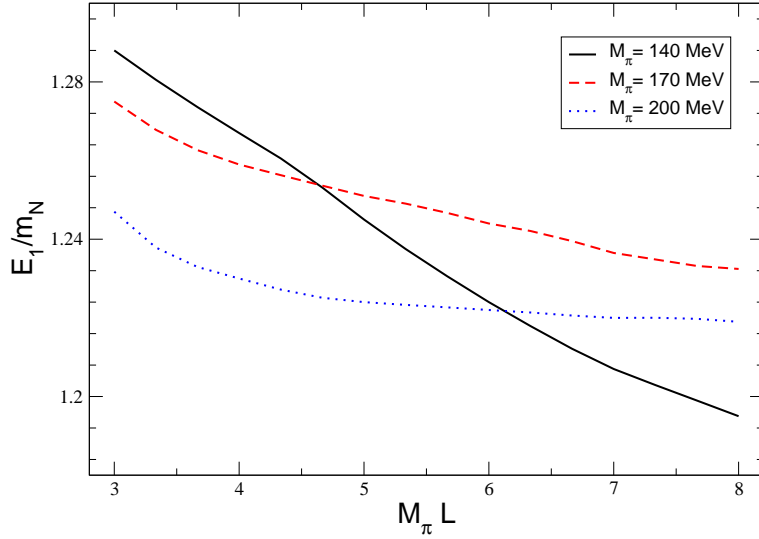


Figure 6: The lowest energy level for different values of M_π and the physical value of $g_{\pi N\Delta}$. The curves correspond to the following values of $\omega_0 \doteq m_\Delta - m_N - M_\pi$: a) solid line: $\omega_0 = 130$ MeV, b) dashed line: $\omega_0 = 78$ MeV, c) dotted line: $\omega_0 = 20$ MeV.

4 Analytic parameterization

The dependence of the energy levels $E_n(L)$ on the parameters m_Δ , $g_{\pi N\Delta}$ and L is given by the numerical solution of Eq. (20). If one implements the above fitting procedure in practice, it would be useful to have a simplified algebraic expression for the energy levels, where the dependence on the parameters is explicit. Below we demonstrate how such an expression can be derived. Starting from Eqs. (21,22,23), we neglect all contributions that are exponentially suppressed in L . Namely, the $\pi\Delta$ loop is neglected altogether as well as various tadpoles. The functions $\tilde{\Sigma}_i(-\omega^2)$, which appear in the self-energy part, are then proportional to the loop function $\tilde{W}_0^N(-\omega^2)$, defined in Eq. (26). Then, Eq. (20) simplifies to

$$m_\Delta - \sqrt{-\omega^2} = -\frac{g_{\pi N\Delta}^2}{F^2} \frac{1}{2\sqrt{-\omega^2}} \left\{ (\sqrt{-\omega^2} + m_N)^2 - M_\pi^2 \right\} \frac{\lambda(-\omega^2, m_N^2, M_\pi^2)}{12\omega^2} \tilde{W}_0^N(-\omega^2). \quad (38)$$

Further, since the Δ is a P -wave state, the lowest singularity in the self-energy corresponds to the contribution of the term with $\mathbf{n}^2 = 1$ (it can be easily checked that the singularity at $\mathbf{n}^2 = 0$ cancels with the factor $\lambda(-\omega^2, m_N^2, M_\pi^2)$ in the numerator). Isolating the singularity at $\mathbf{n}^2 = 1$ in the function $\tilde{W}_0^N(-\omega^2)$, one may write

$$\tilde{W}_0^N(-\omega^2) = \frac{6}{L^3} \frac{E^{(1)}}{2E_N^{(1)}E_\pi^{(1)}} \frac{1}{\omega^2 + (E^{(1)})^2} + \tilde{R}_0^N(-\omega^2), \quad (39)$$

where

$$E_N^{(1)} = \sqrt{m_N^2 + (2\pi/L)^2}, \quad E_\pi^{(1)} = \sqrt{M_\pi^2 + (2\pi/L)^2}, \quad E^{(1)} = E_N^{(1)} + E_\pi^{(1)}, \quad (40)$$

and the function $\tilde{R}_0^N(-\omega^2)$ is regular in the vicinity of $\omega^2 = -(E^{(1)})^2$. Further, Eq. (20) can be rewritten as

$$m_\Delta - \sqrt{-\omega^2} = \frac{g(L)}{E^{(1)} - \sqrt{-\omega^2}} + r(\sqrt{-\omega^2}), \quad (41)$$

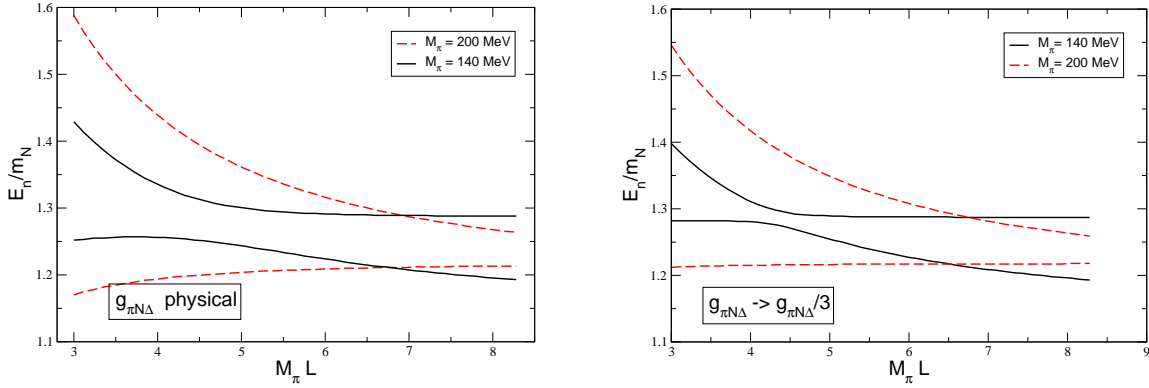


Figure 7: Approximate solution for the first two energy levels, Eq. (43), for physical (left panel) and reduced (right panel) values of the coupling constant $g_{\pi N\Delta}$. The approximate solution qualitatively reproduces the features of the exact solution. Namely, the avoided level crossing is clearly visible in the right panel, as well as an almost stable Δ -state at $M_\pi = 200$ MeV (left and right panels).

where

$$g(L) = \frac{g_{\pi N\Delta}^2}{F^2} \frac{1}{16(E^{(1)})^3} \left\{ (E^{(1)} + m_N)^2 - M_\pi^2 \right\} \lambda((E^{(1)})^2, m_N^2, M_\pi^2) \frac{1}{L^3 E_N^{(1)} E_\pi^{(1)}} \quad (42)$$

and the function $r(\sqrt{-\omega^2})$ is regular at $\sqrt{-\omega^2} = E^{(1)}$.

If now we use the approximation $r(\sqrt{-\omega^2}) = 0$, we arrive at a quadratic equation, whose solution

$$E_{1,2}(L) = \frac{1}{2} \left\{ m_\Delta + E^{(1)} \pm \sqrt{(m_\Delta - E^{(1)})^2 + 4g(L)} \right\} \quad (43)$$

gives the position of the first two energy levels. In Fig. 7 these levels are plotted at the physical value of $g_{\pi N\Delta}$, as well as for the case of a smaller value. It is amusing that such a simple solution reproduces the gross features of the exact solution quite well. For example, the avoided level crossing is clearly visible at smaller values of $g_{\pi N\Delta}$. Finally, we note that in Ref. [16] a very similar equation is derived in a simple two-channel quantum-mechanical model.

The approximate solution, given by Eq. (43), contains an explicit dependence on the parameters L , m_Δ and $g_{\pi N\Delta}$. For this reason, it is easier to use it for performing the fit to the lowest energy levels. Of course, from the quantitative point of view, the quality of the approximation is still not satisfactory. It is however obvious that the accuracy can be systematically improved by including the next nearby singularities as well as regular contributions. We do not display the pertinent formulae here. It is clear that, at the end, the accuracy of the analytic parameterization, which is used to analyze the real lattice data, should be matched to the precision of this data.

5 Conclusions

- a) In this paper we present the results of calculations of the pole structure of the correlator of two Δ -fields in a finite Euclidean box. It has been argued that, calculating the first few energy levels $E_n(L)$ in terms of the resonance parameters m_Δ and $g_{\pi N\Delta}$ within the SSE and fitting the lattice data at finite volume, an extraction of these parameters at a reasonable accuracy may be possible. This statement constitutes the main result of the present paper.

- b) The main question that remains is, how the result will be affected by higher-order corrections in the chiral expansion. It can be for instance shown that, parameterizing pion-nucleon scattering matrix by the pure s -channel Δ -pole term, Eq. (20) can be rewritten in a form similar to the Lüscher's master formula, which expresses the displacement of an energy level through the scattering phase shift. The higher-order corrections in the SSE contribute to the non-resonant background and are expected to be moderate. Of course, such heuristic arguments can not be a real substitute of explicit calculations. Note that such calculations at $O(\epsilon^4)$ are already in progress and the results will be reported elsewhere, including a detailed error analysis in SSE at this order [40]. One expects that these calculations shed light on the question of the convergence of the chiral expansion.
- c) Our approach is closely related to the method proposed originally by Lüscher and developed in number of subsequent publications [12–16,25]. Note, however, that the Lüscher formula, relating the energy levels of a system in a finite volume to the scattering phase shifts, is valid in general beyond the chiral expansion, thus avoiding the above-mentioned problem of convergence. On the other hand, our result contains an explicit parameterization of the energy levels in terms of m_Δ , $g_{\pi N\Delta}$ and can be used, in addition, to study the quark mass dependence of the energy levels. This is important because the first lattice data which will appear below πN threshold, will probably still correspond to the pion mass higher than the physical value.

We now note that, due to the condition $M_\pi L \gg 1$, the characteristic 3-momenta of the system $p \ll M_\pi$ and the non-relativistic approach must be applicable – the processes with a mass gap $\sim M_\pi$ or higher are suppressed exponentially. One therefore expects that, for a sufficiently large L these two approaches overlap and the results are complementary to each other. At present, we are investigating the problem in detail within non-relativistic EFT, aiming to explicitly demonstrate this relationship that, in turn, will enable one to choose an optimum strategy for determining the resonance parameters from the lattice data in the future [41].

Acknowledgments:

The authors would like to thank G. Colangelo, J. Gasser, C. Haefeli, M. Savage, G. Schierholz, R. Sommer and U.-J. Wiese for interesting discussions.

References

- [1] C. M. Maynard and D. G. Richards [UKQCD Collaboration], Nucl. Phys. Proc. Suppl. **119** (2003) 287 [arXiv:hep-lat/0209165].
- [2] D. G. Richards, M. Göckeler, R. Horsley, D. Pleiter, P. E. L. Rakow, G. Schierholz and C. M. Maynard [LHPC Collaboration], Nucl. Phys. Proc. Suppl. **109A** (2002) 89 [arXiv:hep-lat/0112031].
- [3] C. Gattringer *et al.* [BGR Collaboration], Nucl. Phys. B **677** (2004) 3 [arXiv:hep-lat/0307013].
- [4] S. Sasaki, Prog. Theor. Phys. Suppl. **151** (2003) 143 [arXiv:nucl-th/0305014].
- [5] S. Sasaki, T. Blum and S. Ohta, Phys. Rev. D **65** (2002) 074503 [arXiv:hep-lat/0102010].
- [6] J. M. Zanotti *et al.* [CSSM Lattice Collaboration], Phys. Rev. D **65** (2002) 074507 [arXiv:hep-lat/0110216].
- [7] W. Melnitchouk *et al.*, Phys. Rev. D **67** (2003) 114506 [arXiv:hep-lat/0202022].
- [8] L. Zhou and F. X. Lee, Phys. Rev. D **74** (2006) 034507 [arXiv:hep-lat/0604023].

- [9] K. Sasaki and S. Sasaki, Phys. Rev. D **72** (2005) 034502 [arXiv:hep-lat/0503026].
- [10] C. McNeile, arXiv:hep-lat/0307027.
- [11] D. B. Leinweber, W. Melnitchouk, D. G. Richards, A. G. Williams and J. M. Zanotti, Lect. Notes Phys. **663** (2005) 71 [arXiv:nucl-th/0406032].
- [12] M. Lüscher, Commun. Math. Phys. **105** (1986) 153.
- [13] M. Lüscher, Nucl. Phys. B **354** (1991) 531.
- [14] M. Lüscher, Nucl. Phys. B **364** (1991) 237.
- [15] M. Lüscher, DESY-88-156 *Lectures given at Summer School 'Fields, Strings and Critical Phenomena', Les Houches, France, Jun 28 - Aug 5, 1988*
- [16] U.-J. Wiese, Nucl. Phys. Proc. Suppl. **9** (1989) 609.
- [17] K. Rummukainen and S. A. Gottlieb, Nucl. Phys. B **450** (1995) 397 [arXiv:hep-lat/9503028].
- [18] N. H. Christ, C. Kim and T. Yamazaki, Phys. Rev. D **72** (2005) 114506 [arXiv:hep-lat/0507009].
- [19] C. H. Kim, C. T. Sachrajda and S. R. Sharpe, Nucl. Phys. B **727** (2005) 218 [arXiv:hep-lat/0507006].
- [20] T. A. DeGrand, Phys. Rev. D **43** (1991) 2296.
- [21] C. Michael, Nucl. Phys. B **327** (1989) 515.
- [22] R. D. Loft and T. A. DeGrand, Phys. Rev. D **39** (1989) 2692.
- [23] L. Lellouch and M. Lüscher, Commun. Math. Phys. **219** (2001) 31 [arXiv:hep-lat/0003023].
- [24] T. Yamazaki and N. Ishizuka, Phys. Rev. D **67** (2003) 077503 [arXiv:hep-lat/0210022].
- [25] S. R. Beane, P. F. Bedaque, A. Parreno and M. J. Savage, Nucl. Phys. A **747** (2005) 55 [arXiv:nucl-th/0311027].
- [26] S. R. Beane, P. F. Bedaque, A. Parreno and M. J. Savage, Phys. Lett. B **585** (2004) 106 [arXiv:hep-lat/0312004].
- [27] S. R. Beane, P. F. Bedaque, T. C. Luu, K. Orginos, E. Pallante, A. Parreno and M. J. Savage, arXiv:hep-lat/0612026.
- [28] S. R. Beane, P. F. Bedaque, K. Orginos and M. J. Savage, Phys. Rev. Lett. **97** (2006) 012001 [arXiv:hep-lat/0602010].
- [29] S. Sasaki and T. Yamazaki, arXiv:hep-lat/0610081.
- [30] T. R. Hemmert, B. R. Holstein and J. Kambor, J. Phys. G **24** (1998) 1831 [arXiv:hep-ph/9712496].
- [31] W. Detmold and M. J. Savage, Phys. Lett. B **599** (2004) 32 [arXiv:hep-lat/0407008].
- [32] P. F. Bedaque, H. W. Grißhammer and G. Rupak, Phys. Rev. D **71** (2005) 054015 [arXiv:hep-lat/0407009].
- [33] A. Ali Khan *et al.* [QCDSF-UKQCD Collaboration], Nucl. Phys. B **689** (2004) 175 [arXiv:hep-lat/0312030].
- [34] S. R. Beane, Phys. Rev. D **70** (2004) 034507 [arXiv:hep-lat/0403015].

- [35] G. Colangelo, A. Fuhrer and C. Haefeli, Nucl. Phys. Proc. Suppl. **153** (2006) 41 [arXiv:hep-lat/0512002].
- [36] V. Bernard, T. R. Hemmert and U.-G. Meißner, Phys. Lett. B **622** (2005) 141 [arXiv:hep-lat/0503022].
- [37] J. Gasser and H. Leutwyler, Nucl. Phys. B **307** (1988) 763.
- [38] M. Lüscher, Commun. Math. Phys. **104** (1986) 177.
- [39] G. Höhler, in Landolt-Börnstein, vol. 9 b2, ed. H. Schopper (Springer, Berlin, 1983).
- [40] V. Bernard, D. Hoja, U.-G. Meißner and A. Rusetsky, in progress.
- [41] V. Bernard, M. Lage, U.-G. Meißner and A. Rusetsky, in progress.